The role of parthanatos in the pathomechanism of endothelial dysfunction and heart failure

PhD thesis

Tamas Barany M.D.

Doctoral School of Basic and Translational Medicine
Semmelweis University

Supervisor:
Mária Eszter Horváth M.D., Ph.D., assistant professor
Consultant: Endre Zima M.D., Ph.D., associate professor

Official rewievers:
Viktor Horváth M.D., Ph.D., assistant professor
Zsófia Verzár M.D., Ph.D., associate professor
Head of the Final Examination Committee:
István Pénzes M.D., D.Sc., professor emeritus
Members of the Final Examination Committee:
Ákos Zsembery M.D., Ph.D., associate professor
Hajnalka Bálint M.D., Ph.D.

Budapest
2019

1. INTRODUCTION

Poly(ADP-ribose) polymerase-1 (PARP) is the major nuclear isoform of enzyme family, with multiple regulatory functions. Upon activation, mainly by DNA single-strand breaks, it cleaves NAD^+ into nicotinamide and ADP-ribose, forms long branches of ADP-ribose polymers, and binds them to several nuclear target proteins (PARylation). PARP activation exerts its physiological and pathological effects via two principal mechanisms. On one hand, it PARylates acceptor proteins including histones, transcription factors. PARylation contributes to DNA repair and to the regulation of gene expression. The protein expression of various proinflammatory mediators is regulated by PARP at the transcriptional level. On the other hand, oxidative-nitrative stress-induced overactivation of PARP consumes NAD^+ and consequently ATP, culminating in cell dysfunction and necrotic cell death. Poly(ADP-ribosyl)ation was detected in case of oxidative-nitrative stress-induced DNA damage and was shown to play a regulatory role in different cell death pathways. During caspase-dependent apoptosis, PARP-1 is cleaved by caspases preventing further loss of NAD^+ and providing energy for the apoptotic processes. PAR accumulation can induce a form of caspase-independent death triggering the translocation of mitochondrial factors, including apoptosis inducing factor (AIF). Pathogenic PAR polymer translocates to the mitochondria from the nucleus to mediate AIF release. AIF translocation to the nucleus promotes chromatin condensation and DNA degradation. This crosstalk between nucleus and mitochondria is the key point in a special cell death pathway called parthanatos.

In various models of diabetes mellitus and heart failure, oxidative-nitrative stress and PARP activation have been shown

to play important roles in the pathomechanism. In response to hyperglycaemia the generation of multiple reactive species occurs in endothelial cells promoting vascular dysfunction. Reactive radicals interact with NO and reduce its bioavailability, which contributes to the development of endothelial dysfunction. Although the role of persistent hyperglicaemia has been demonstrated in a number of studies, the relevance of glicaemic fluctuation is less clear in the development of diabetic vascular complications.

In the development of heart failure, reactive radicals also have a prominent role. In heart failure with preserved ejection fraction, myocardial dysfunction and remodeling are driven by endothelial inflammation and free radicals. In heart failure with reduced ejection fraction, oxidative-nitrative stress originates in the cardiomyocytes because of ischemia, infection, or toxic agents. More experimental studies provided increasing number of evidence of increased oxidative-nitrative stress-induced PARP activation in the development of cardiac dysfunction. But there are only few human studies that investigated the role of PARP in heart failure.

2. OBJECTIVES

The concept of parthanatos was introduced for a few years, but the PARP enzyme has been examined for decades. Many studies have demonstrated that PARP activation caused by oxidative-nitrative stress plays a central role in various diseases. Our aim was to investigate PARP activation in cardiovascular morbidities. We examined the possible relationship between markers of parthanatos detected in various tissues and endothelial dysfunction induced by glycemic oscillation in an animal model or human chronic heart failure.

2.1 Endothelial dysfunction and parthanatos in glicaemic oscillation

We have investigated:

1. whether glicaemic fluctuation affect endothel-dependent relaxation causing endothelial dysfunction.
2. the changes of local and systemic oxidative-nitrative stress due to oscillating glucose.
3. whether there is increased activity of PARP in condition of fluctuation of blood glucose level.

2.2 Parameters of heart failure and parthanatos

We have investigated:

1. whether there is parthanatos phenomenon (oxidative-nitrative stress, PARP activation, and AIF translocation) in blood components of patients with chronic heart failure.
2. whether parthanatos demonstrates any correlation with parameters of heart failure or clinical features.

3. METHODS

3.1 Diabetic animal model

Nineteen age-matched male Wistar rats (Toxicoop, Budapest, Hungary) weighing 380-480 g were administered 70 mg/kg streptozotocin (STZ) i.v. From the 14th day we started insulin therapy: the first group received 60 U/kg of intermediate-acting (lente) glargine insulin (Sanofi Aventis, Paris, France) s.c. daily, every afternoon at 17:00 hours (DM with good glycaemic control [DM-GGC] animals, n=6). The second group was treated with 60 U/kg long-acting (ultralente) insulin (Novo Nordisk, Bagsvaerd, Denmark) s.c. on every second day at 17:00 hours (DM with poor glycaemic control [DM-PGC] animals, n=7). Six diabetic animals were left untreated (DM group). The age-matched control group received the vehicle of the drugs (control, n=7). After 10 days of insulin treatment, blood glucose levels of every rat were monitored for 48 h; the collection of samples started immediately before insulin dosage and was repeated every 6 h. After 2 weeks of insulin treatment, the rats were anaesthetised with i.p. thiopental sodium and were killed. Thoracic aorta, blood and bone marrow were harvested for further measurements.

All investigations conformed to the Guide for the Care and Use of Laboratory Animals published by the National Institutes of Health (NIH Publication No. 85-23, Revised 1985), and were approved by the local Animal Use Committee.

3.2 Human, chronic heart failure

20 patients between the age of 50 and 70 years with known chronic heart failure (CHF) having clinically stable cardiopulmonary state (NYHA (New York Heart Association) II-III) were enrolled at the Heart and Vascular Center of

Semmelweis University, Budapest, Hungary. Heart failure was diagnosed according to the actual guideline of the European Society of Cardiology (ESC) published in 2016. CHF diagnosis was verified by the reduced systolic function defined as ejection fraction (EF) below 40%. NYHA stages were also determined according to the ESC guideline. Volunteers matched by age, body mass index, and cardiovascular risk factors (smoking, diabetes mellitus, hypertension, and ischemic heart disease (IHD)) with normal systolic function served as controls (n=15).

All procedures complied with the Helsinki Declaration of the World Medical Association and were approved by the institutional and regional ethics committee of Semmelweis University (7268-0/2011-EKU). Written informed consent was acquired from all participants.

3.3 Vascular function in glicaemic oscillation

The thoracic aorta was cleared from periadventitial fat and cut into 2–3 mm width rings, mounted in organ baths filled with warmed (37°C) and oxygenated (95% O2, 5% CO2) Krebs solution (CaCl2 1.6 mmol/l; MgSO4 1.17 mmol/l; EDTA 0.026 mmol/l; NaCl 130 mmol/l; NaHCO3 14.9 mmol/l; KCl 4.7 mmol/l; KH2PO4 1.18 mmol/l; glucose 11 mmol/l). Isometric tension was measured with isometric transducers and registered (Kipp & Zonen BD300, Bohemia, NY, USA). A tension of 1 g was applied and the rings were equilibrated for 60 min. After equilibration the contractile response of arterial rings to a depolarising solution of a modified Krebs solution enriched in K^+ was first tested to evaluate their functional integrity. Increasing doses of phenylephrine (10^{-8}- 3×10^{-5} mol/l) were used to determine contraction capability. Rings were pre-contracted with phenylephrine (10^{-6} mol/l) and then dose–response curves to acetylcholine (1×10^{-8}- 3×10^{-5} mol/l) were

constructed. Increasing doses of sodium nitroprusside (1×10^{-8}-1×10^{-5} mol/l) were used to check NO-dependent vasodilatation. Experiments were conducted in eight to ten rings (four or five animals) in each experimental group. Contractile responses to phenylephrine were expressed as a percentage of K^+-induced contractions. Relaxations were expressed as a percentage relative to the pre-contraction achieved by phenylephrine.

3.4 Examination of parthanatos

3.4.1 Biochemistry

Fasting blood samples were collected from all subjects for C-reactive protein (CRP), N-terminal probrain-type natriuretic peptide (pro-BNP), oxidative-nitrative stress, PARP activity, and AIF translocation measurements.

Plasma total peroxide level (PRX) was measured by Oxystat kit according to the user's manual. Total plasma antioxidant capacity (TAC) was measured by OxiSelect™ TAC Assay Kit according to the user's manual. Absorption was detected by Bio Tek Powerwave XS Spectrophotometer. Oxidative stress index (OSI) is given as the ratio of total peroxide and TAC.

3.4.2 Immunohistochemistry

In animal model thoracic aorta, and bone marrow were harvested for immunologic measurements. In patients circulating mononuclear leukocytes were isolated by gradient centrifugation. Anti-nitrotyrosine (NT) rabbit polyclonal antibody (4°C, overnight) was used to stain 3-nitrotyrosine, the marker of tyrosine nitration. The level of lipidperoxidation was estimated by using anti-4-hydroxy-2-noneal (HNE) rabbit polyclonal antibody (4°C, overnight). The detection of PAR was performed by using mouse monoclonal anti-PAR antibody (4°C,

overnight). AIF translocation were estimated by immunohistochemical staining with anti-AIF rabbit polyclonal (4°C, overnight) antibodies. Secondary labelling was achieved by using biotinylated anti-mouse horse or anti-rabbit goat antibody (30 min.). Avidin-horseradish peroxidase complex and brown-colored diaminobenzidine (DAB) or black-colored nickel-enhanced DAB (Vector) were used to visualize specific labeling. Blue-colored hematoxyilin or red-colored Nuclear Fast Red (NFR) was used as counterstain.

3.4.3 Western blot analysis

After protein isolation from rat aorta tissue, proteins were separated by 10–15% sodium dodecyl sulphate-polyacrylamide gel electrophoresis (SDS-PAGE) according to the manufacturers' protocol (Invitrogen, Carlsbad, CA, USA). Following electrophoresis, proteins were transferred to an immobilon polyvinylidine fluoride (PVDF) membrane (Xcell II blot, Invitrogen). For the determination of PARylation primary antibody against PAR (monoclonal antibody; 1:2000, overnight at 4°C) was used. The membranes were then incubated with horseradish peroxidase-conjugated anti-mouse secondary antibodies at a dilution of 1:2000 for 1 hour (at room temperature). The blots were then developed using the enhanced chemiluminescence method. Densitometry was performed by ImageJ software (National Institutes of Health, Bethesda, MD, USA).

3.4.4 Flow cytometry

Circulating leucocytes were isolated from whole blood using Histopaque-1083 according to the Users' Manual. After the fixation and permeabilisation of the cells with a Cytofix/Cytoperm Fixation/Permeabilization Solution Kit,

monoclonal mouse anti-PAR antibody (30 min, 4°C) was used as primary antibody. Purified mouse IgG3κ isotype control (anti-keyhole limpet haemocyanin) antibody served as isotype control. FITC-conjugated anti-mouse immunoglobulin specific polyclonal antibody (multiple absorptions) (30 min, 4°C) was used as secondary antibody.

3.5 Statistical Analysis

Results are expressed as mean, standard deviation (SD) or standard error of mean (SEM) for normally distributed variables and median (interquartile range) for non normally distributed variables. Variables that violated the normality assumption were log-transformed before using them in the statistical models. One- and two-way ANOVA (vascular function tests), Tukey and Bonferroni post hoc tests were used to compare more experimental groups. Participants' characteristics by study group were compared using two-tailed independent samples t-test. The distribution of categorical variables in the different groups was compared by chi-square test. The possible relationship between clinical parameters and oxidative-nitrative stress, PARP activation, AIF translocation in the study cohort, and among CHF patients was examined by Pearson's correlation test and linear regression models. In case of multiple significant correlations in the CHF group, multivariate linear regression models were implemented.

4. RESULTS

4.1 Endothel dysfunction in glicaemic oscillation

4.1.1 Blood glucose fluctuations in experimental animal model

The blood glucose levels of the untreated control rats showed only a very slight circadian rhythm between 7.2±0.8 mmol/l and 8.5±0.3 mmol/l. The animals in the untreated DM group were markedly hyperglycaemic; their blood glucose levels fluctuated between 28.8±5.6mmol/l and 46.4±4.2 mmol/l. DM-GGC animals, similarly to untreated control rats, showed only slight circadian changes between 5.6±1.1 mmol/l and 11.5±8.4 mmol/l. Although this fluctuation due to insulin treatment does not follow the circadian changes of healthy animals, the blood glucose levels of these animals never exceeded the normal levels. In the DM-PGC group, blood glucose levels changed between 11.3±1.5 and 43.4±3.1 mmol/l (figure 1).

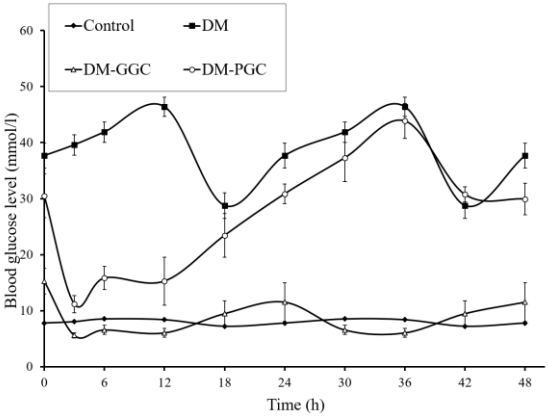

Figure 1: Blood glucose profiles of control rats, DM rats and DM rats with PGC or GGC (values are means±SEM)

4.1.2 Endothelium-dependent relaxation and fluctuating blood sugar levels

Experiments conducted on vascular rings showed a marked impairment in the phenylephrine-induced contractions and in the acetylcholine-induced, endothelium dependent relaxations in the DM-PGC group (Figure 2/a, 2/b). The latter effect is probably related to a reduced ability of the vascular endothelium to produce NO in response to acetylcholine, and not due to a reduced ability of the vascular smooth muscle to relax to NO, because the relaxant effect of the NO donor sodium nitroprusside was not attenuated.

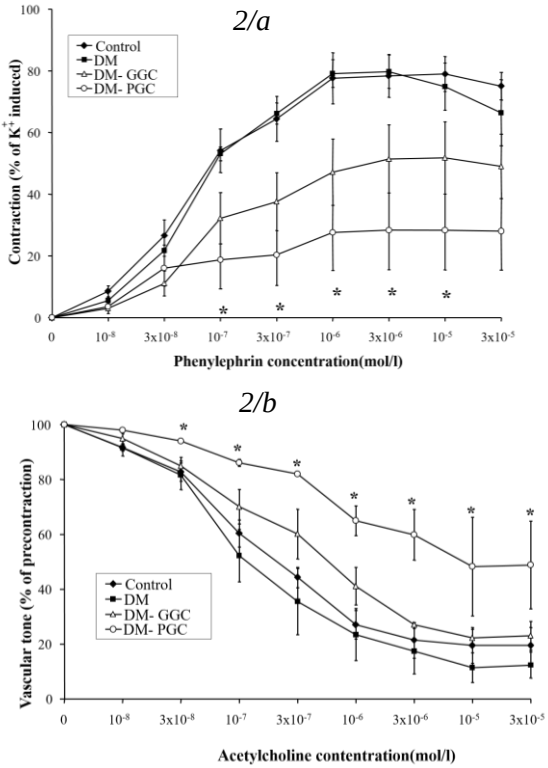

*Figure 2/a, 2/b: Effects of insulin treatment on contractile and endothelium dependent relaxant function of the thoracic aorta (values are means±SEM, *p<0.05 DM-PGC vs. control)*

4.1.3 Oxidative-nitrative stress in glicaemic oscillation

The immunohistochemical analysis of bone marrow smears showed increased numbers of NT-positive cells in DM and DM-PGC groups compared with the control group (8.9±0.6% and 8.4±0.6% vs 3.7±0.9%, respectively, $p<0.01$) (Figure 3).

Immunohistochemical analysis showed a stronger HNE staining in the endothelium of the DM-PGC animals, although the differences did not reach the level of significance (control: 3.4±0.3, DM: 5.1±1.3, DM-GCC: 4.3±1.2, DM-PGC: 5.5±1.3). NT immunohistochemistry did not reveal any significant difference between the experimental groups.

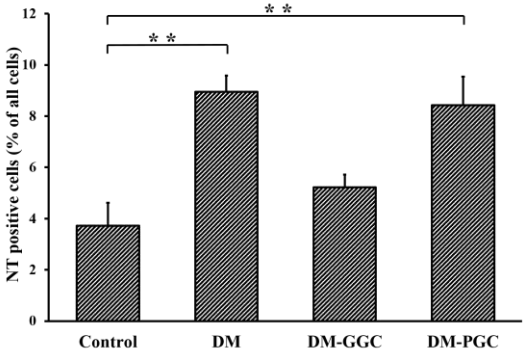

*Figure 3: Percent of NT-positive bone marrow cells (values are means+SEM, **p<0.01)*

4.1.4 PARP activation in tissues and circulating leukocytes

The immunohistochemical analys is of bone marrow smears demonstrated strongest PAR staining in the DM group. Although in diabetic animals, insulin treatment in DM-GGC

decreased PAR positivity, in DM-PGC it did not exert a similar effect.

The most pronounced PARP activity was localized in the endothelium of the DM-PGC animals (4.8±0.7 vs DM-GGC: 2.0±0.3; Figure 4). When western blots involving whole aortic homogenates were tested, the amount of poly (ADP-ribosyl)ated proteins was highest in the untreated diabetic group, and was lower in the diabetic animals treated with short- or long-lasting insulin. However, there was a 50 kDa poly (ADP-ribosyl)ated band that was more pronounced in the poorly insulin controlled diabetic animals than in the diabetic animals without insulin treatment (Figure 5).

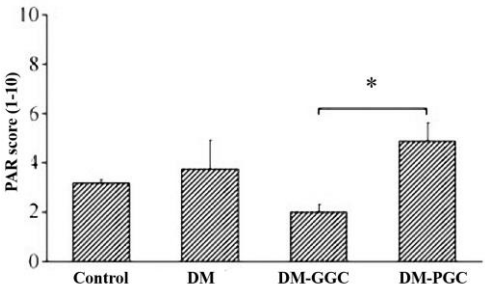

Figure 4: PAR score of the aortic wall
*(values are means+SEM, *p<0.01)*

There was a marked increase in PARP activity in the circulating leucocytes in the DM rats, as evidenced by flow cytometry (Figure 6/a, 6/b). However, insulin therapy reduced PARP activity, regardless of the mode of therapy, whether it developed optimal treatment or fluctuating blood glucose.

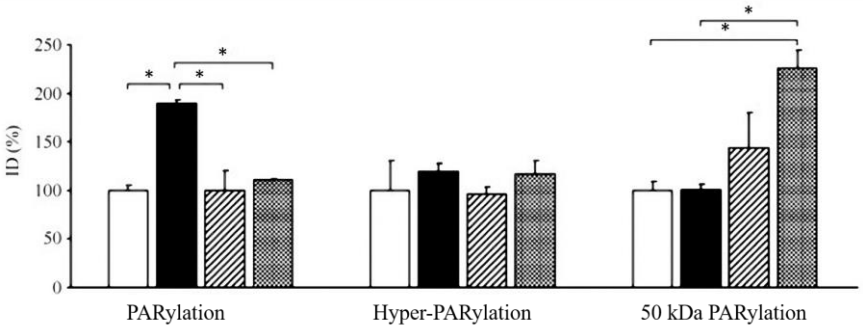

*Figure 5: Densitometric analysis of the PAR western blots of aortic walls. ID, relative image density (% of untreated control, which is considered 100%), white columns, control rats; black columns, DM rats; hatched columns, DM-GGC rats, grey columns, DM-PGC rats, values are means+SEM, *p<0.05)*

6/a

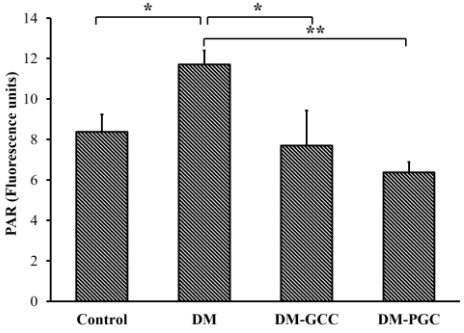

6/b

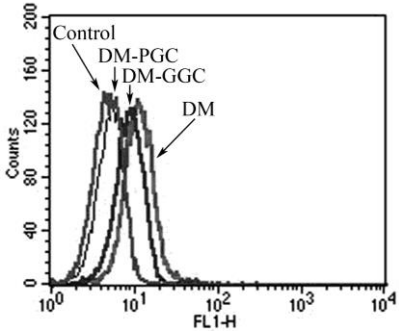

*Figure 6/a Flow cytometric analysis of circulating leucocytes. (values are means+SEM. *p<0.05, **p<0.01)*
Figure 6/b Representative flow cytometric measurement of PAR-stained circulating lymphocytes. FL1-H shows the fluorescence intensity of cells. 'Counts' means the number of cells having certain fluorescence intensities.

4.2 Parameters of heart failure and parthanatos

4.2.1 Clinical parameters and anamnestic data

20 patients with chronic heart failure (CHF) and 15 controls were enrolled. The gender composition of the two groups was similar. Both age and body mass index of the two study groups were also comparable. There was no significant difference concerning the prevalence of hypertension, diabetes mellitus, ischemic heart disease, and smoking habit. The level of the inflammatory marker CRP was not significantly different in the study cohorts. Ejection fraction was significantly lower (60.0±5.3 % vs 24.9±5.9 %, $p<0.01$); left ventricular end systolic (31.4±5.1 mm vs 54.0±10.6 mm, $p<0.01$) and end diastolic diameters (48.2±4.6 mm vs 63.0±11.1 mm, $p<0.01$) were significantly higher in the diseased group. The level of pro-BNP was markedly increased in CHF patients (148.4 [47.9; 178.0] pg/mL vs 2338.5 [1475.6; 4597.5] pg/mL, $p<0.01$).

4.2.2 Oxidative, Nitrative Stress, PARP Activation, and AIF Translocation in Blood Components

Plasma PRX level was significantly increased in the CHF group indicating that these patients had more intensive oxidative stress compared to controls. On the other hand, TAC was not significantly elevated in CHF patients ($p=0.066$). After calculating OSI, we also found a non significant elevation of this parameter among CHF patients ($p=0.059$). Similarly to PRX, cellular oxidative stress assessed by leukocyte HNE immunostaining intensity was also significantly increased in the CHF group compared to controls. We observed significant elevation in leukocyte NT staining intensity too, which may suggest an elevated nitrosative environment in CHF. The degree of PAR labeling in circulating mononuclear cells, reflecting the PARP activity in these cells, was significantly elevated in the

disease group. Furthermore, in the CHF group, the number of AIF-positive cells was significantly increased compared to the control group (Figure 7).

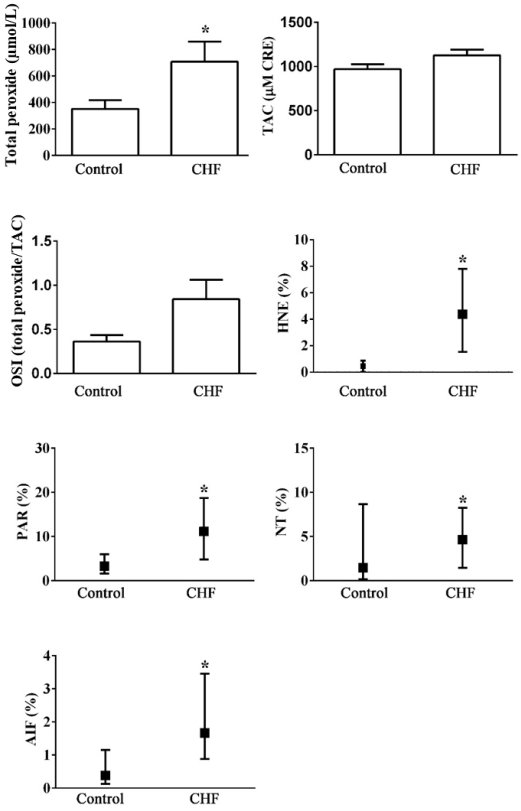

*Figure 7: Parthanatos in blood components (mean+SEM for normally distributed variables and median±interquartile range for non normally distributed variables: HNE, NT, PAR, and AIF, *p<0.05)*

4.2.3 Correlation of parthanatos with cardiac function and clinical features

Examining the correlation between oxidative-nitrative stress, PARP activation, AIF translocation, and the used indicators of cardiac function, such as ejection fraction and pro-BNP levels in all study subjects, revealed a significant positive correlation of the latter with all the following parameters: PRX level, OSI, leukocyte HNE, tyrosine nitration, PARylation, and AIF translocation. EF negatively correlated with same parameters. Analysing CHF group only showed that plasma PRX level, OSI, and PARP activity positively correlate with pro-BNP levels of the chronic heart failure patients (Figure 8).

In the whole study cohort, plasma PRX level and OSI positively correlated with the presence of IHD ($R=0.587$, $p<0.01$ and $R=0.573$, $p<0.01$, resp.) and smoking habit ($R=0.552$, $p<0.01$ and $R=0.525$, $p<0.01$, resp.) In the CHF group, total plasma peroxide level and OSI positively correlated with the presence of IHD ($R=0.676$, $p<0.05$ and $R=0.687$, $p<0.05$). The multivariate regression analysis showed that serum pro-BNP and IHD are independent determinants of plasma total peroxide level, and together they can explain the 97.7% of its variability.

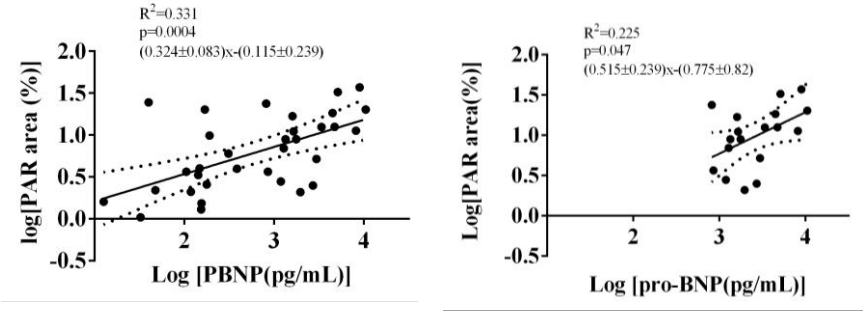

Figure 8: Linear regression of pro-BNP and leukocyte PARylation

5. CONCLUSIONS

1. Impairment of endothelial dependent relaxation of aorta induced by glycemic swings was detected. According to our results not only chronic hyperglicemia but also the glucose fluctuations can play role in the development of cardiovascular complications of diabetes mellitus.
2. Our study showed the presence of free radicals resulting from glucose oscillation similarly to the results of previous studies. Significant nitrotyrosine staining of bone marrow was demonstrated in condition of glycaemic fluctuation.
3. Glicaemic oscillation caused marked PARP activation in the endothelial layer. During western blots the amount of poly(ADP-ribosyl)ated proteins was highest in the untreated diabetic group. There was a 50 kDa poly(ADP-ribosyl)ated band that was more pronounced in the poorly insulin controlled diabetic animals. Due to adequate insulin treatment PARP activation was significantly reduced in the bone marrow cells, endothelium and circulating leukocytes. Our results suggest that besides hyperglycemia, fluctuations of glucose levels may also affect PARP activation.
4. Peripheral blood markers of oxidative-nitrosative stress, PARP activation, and AIF translocation were significantly higher in the heart failure group, which refers to the phenomenon of parthanatos.
5. In all subjects, significant correlation of both pro-BNP levels and impairment of ejection fraction was showed with the markers of parthanatos. Among heart failure patients, positive correlation of pro-BNP with PARP activation and oxidative stress was also found. According to our results, pro-BNP and coronary artery disease showed independent correlations to the degree of oxidative stress.

6. BIBLIOGRAPHY OF THE CANDIDATE'S PUBLICATIONS

6.1 Publications related to the thesis

1. **Barany T**, Simon A, Szabo G, Benko R, Mezei Z, Molnar L, Becker D, Merkely B, Zima E, Horvath EM. (2017) Oxidative Stress-Related Parthanatos of Circulating Mononuclear Leukocytes in Heart Failure. Oxid Med Cell Longev, 2017: 1249614. **IF: 4,936**

2. Horvath EM, Benko R, Kiss L, Muranyi M, Pek T, Fekete K, **Barany T**, Somlai A, Csordas A, Szabo C. (2009) Rapid 'glycaemic swings' induce nitrosative stress, activate poly(ADP-ribose) polymerase and impair endothelial function in a rat model of diabetes mellitus. Diabetologia, 52: 952-961. **IF: 6,551**

6.2 Publications not related to the thesis

1. Toth-Zsamboki E, Horvath E, Vargova K, Pankotai E, Murthy K, Zsengeller Z, **Barany T**, Pek T, Fekete K, Kiss RG, Preda I, Lacza Z, Gero D, Szabo C. (2006) Activation of poly(ADP-ribose) polymerase by myocardial ischemia and coronary reperfusion in human circulating leukocytes. Mol Med, 12: 221-228. **IF:2,708**

2. **Bárány T**, Muk B, Osztheimer I, Szilágyi Sz, Molnár L, Kutyifa V, Becker D, Gellér L, Merkely B, Zima E. (2011) Pacemaker-implantált betegek telekardiológiai utánkövetése – Hazai tapasztalatok a Home Monitoring rendszerrel. Card Hu, 41: 231-238.

3. Boriani G, Da Costa A, Ricci RP, Quesada A, Favale S, Iacopino S, Romeo F, Risi A, Mangoni di S Stefano L, Navarro

X, Biffi M, Santini M, Burri H, MORE-CARE Investigators (**Barany T**). (2013) The MOnitoring Resynchronization dEvices and CARdiac patiEnts (MORE-CARE) randomized controlled trial: phase 1 results on dynamics of early intervention with remote monitoring. J Med Internet Res, 15: e167. **IF: 4,669**

4., **Bárány T**, Szilágyi Sz, Molnár L, Gellér L, Hüttl K, Merkely B, Zima E. (2013) Carotis-intervenciót követő hemodinamikai instabilitás kezelése. Card Hu, 43: 8-10.

5. Csobay-Novak C, **Barany T**, Zima E, Nemes B, Sotonyi P, Merkely B, Huttl K. (2015) Role of stent selection in the incidence of persisting hemodynamic depression after carotid artery stenting. J Endovasc Ther, 22: 122-129. **IF: 3,128**

6. Zima E, Dér G, **Bárány T**, Németh T, Molnár L, Osztheimer I, Szilágyi Sz, Király Á, Papp R, Tarjányi Z, Kiss O, Kosztin A, Nagy Klaudia V, Muk B, Kiss B, Nagy A, Bokrosné Magyar E, Csobánné Oláh Cs, Gellér L, Merkely B. (2017) A telemonitorozás lehetőségei beültethető kardiális elektronikus eszközökkel. Card Hu, 47: 281-289.

7. Papai G, Csato G, Racz I, Szabo G, **Barany T**, Racz A, Szokol M, Sarman B, Edes IF, Czuriga D, Kolozsvari R, Edes I. (2018) The transtelephonic electrocardiogram-based triage is an independent predictor of decreased hospital mortality in patients with ST-segment elevation myocardial infarction treated with primary percutaneous coronary intervention. J Telemed Telecare, 1357633X18814335. **IF: 3.046**